

Growth mechanism and photoluminescence property of flower-like ZnO by hydrothermal method

Bo Cao^{1, 2*}, Irsa Rasheed¹

¹School of Nuclear Science and Engineering, North China Electric Power University, Beijing, 102206, China,

²Department of Atmospheric and Oceanic Sciences, University of California, Los Angeles, CA, 90095, USA

With high stability, good optical characteristics, and unique electrical properties, ZnO nanostructures has been widely used in the vast fields. Because of its good performance in photoluminescence and photocatalysis, the three-dimensional (3D) flower-like nanostructure of ZnO has been paid much attention in recent years. In this paper, flower-like ZnO nanostructures formed by nanorods have been successfully synthesized by hydrothermal method. A number of techniques, including X-ray diffraction (XRD), scanning electron microscopy (SEM), and room temperatures photoluminescence (PL) were used to characterize the structural and optical properties of the obtained flower-like nanostructures of ZnO. The results indicate that the samples are highly crystalline with the wurtzite hexagonal phase, the average crystallite size of the sample was about 44 nm. A uniform flower-like three-dimension (3D) microstructures with diameters in the range of 3-5 μm was assembled by several densely arranged sword-like ZnO nanorods as "petals" with lengths in the range of 400-650 nm and a width in the range of 50-130 nm. The Photoluminescence spectrum (PL) showed that the as-synthesized flower-like ZnO showed ultraviolet emission (UV) at 381 nm and the visible emission band ranging from 450 nm to 750 nm, respectively. In addition, the growth mechanism of the flower-like ZnO was discussed.

Keywords: Zinc oxide, flower-like nanostructures, Photoluminescence spectrum (PL), growth mechanism, hydrothermal method

INTRODUCTION

Zinc oxide (ZnO) is an important n-type semiconductor metal oxide with a wide band gap (3.37 eV) and large exciton binding energy (60 meV) at room temperature. Because of high stability, good optical characteristics, and unique electrical properties [1-3], ZnO nanostructures has been widely used in the enormous fields such as solar cells, nano-lasers, piezoelectric devices, etc. [4-9]. The properties of ZnO nanostructures mainly depended strongly on their morphology, specific surface, crystallize size. Up to date, various morphologies of ZnO nanostructures including nanobelts, nanowires, nanorods, nanotubes, and nanoflowers have been demonstrated via thermal evaporation, chemical-vapor deposition (CVD), thermal evaporation, molecular-beam epitaxy (MBE), pulsed-laser deposition (PLD), electrochemical deposition and spray pyrolysis [10-18].

Because of its good performance in photoluminescence and photocatalysis, the three-dimensional (3D) flower-like nanostructure of ZnO has been paid much attention in recent years [19-22]. The low temperature hydrothermal synthesis has been widely used for the growth of ZnO nanostructures, mainly because of its simplicity,

cost effectiveness and the ability to control the shape and dimensions [23-25]. Till now, although flower-like ZnO have been synthesized by hydrothermal method, the growth mechanism and photoluminescence are also still need to be well exploited.

In the present study, the flower-like nanostructures of ZnO were synthesized by hydrothermal method with zinc acetate dehydrate ($\text{Zn}(\text{CH}_3\text{COO})_2 \cdot 2\text{H}_2\text{O}$) and sodium hydroxide (NaOH). The as-synthesized ZnO nanostructures were characterized by X-ray diffraction (XRD), scanning electron microscopy (SEM), and room temperature photoluminescence (PL) spectra.

EXPERIMENT

In this study, ZnO nanostructures sample has been synthesized using chemical methods. All of the raw materials were of analytical grade. First, about 1.32 mg of zinc acetate dehydrate ($\text{Zn}(\text{CH}_3\text{COO})_2 \cdot 2\text{H}_2\text{O}$) was dissolved in 20 ml of deionized water while stirring at room temperature. Then the 9 ml of sodium hydroxide (NaOH) was added gradually to the above solution under continuous stirring at room temperature. After this step, add distilled water to bring volume to 40 ml. The solution was transferred to a Teflon-lined autoclave. The autoclave was sealed and maintained at 160 °C for 12h, and then cooled to room temperature. The white precipitate was

* To whom all correspondence should be sent:
caobo@ncepu.edu.cn

separated by filtration, washed with deionized water and dried in an oven at 60 °C.

Characterization of samples was performed by X-ray diffraction (XRD) analysis and scanning electron microscopy (SEM) measurement. The powder X-ray patterns were carried out using a Philips X'pert automated diffractometer with monochromated Cu K-Alpha radiation of 1.5406 Å. The X-ray tube was operated at a voltage of 45 kV and a current of 40 mA. The peak position and intensities were obtained between 20 °C and 80 °C with a velocity of 0.02 per second. The surface morphologies and structure of the samples were studied by field emission scanning electron microscope (FE-SEM, JSM 6701-F, JEOL, Japan). Room temperature photoluminescence (RT-PL) spectra were measured using a He-Cd laser with the wavelength of 325 nm as the excitation source.

RESULTS AND DISCUSSION

XRD analysis

The XRD pattern of the as-synthesized product is shown in Fig.1. It can be seen that all of the diffraction peaks are in agreement with the JCPDS file of ZnO (JCPDS No. 36-1451). It is confirmed that the samples show wurtzite structure of ZnO belonging to the space group of P63mc (lattice parameters: $a=0.3249$ nm, $c=0.5206$ nm). No impurities could be observed in these patterns. Moreover, the sharp diffraction peaks manifest the high crystallinity of the sample. By using the Bragg's law and the Debye-Scherrer equation, we calculated the average crystallite size of the sample was about 44 nm.

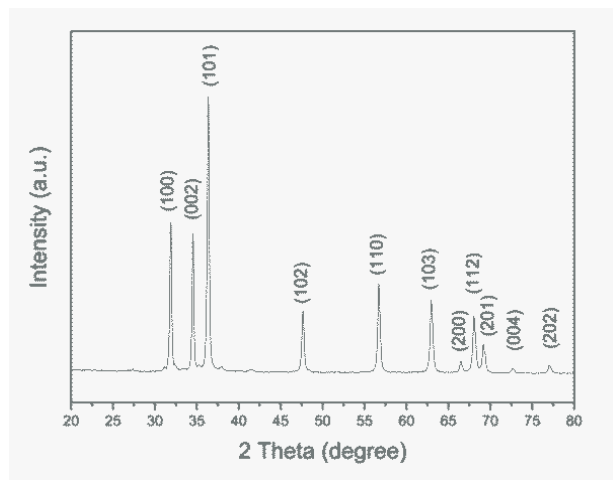


Fig.1. XRD patterns of the synthesized ZnO nanostructures

SEM characterization

Fig.2(a) and Fig.2(b) are the images of flower-like ZnO in low magnification and in high magnification, respectively. It can be seen a uniform flower-like three-dimension (3D) microstructures with diameters in the range of 3-5 μm (Fig.2(a)), assembled by several densely arranged sword-like ZnO nanorods as “petals” with lengths in the range of 400-650 nm (Fig.2(b)); and a width in the range of 50-130 nm.

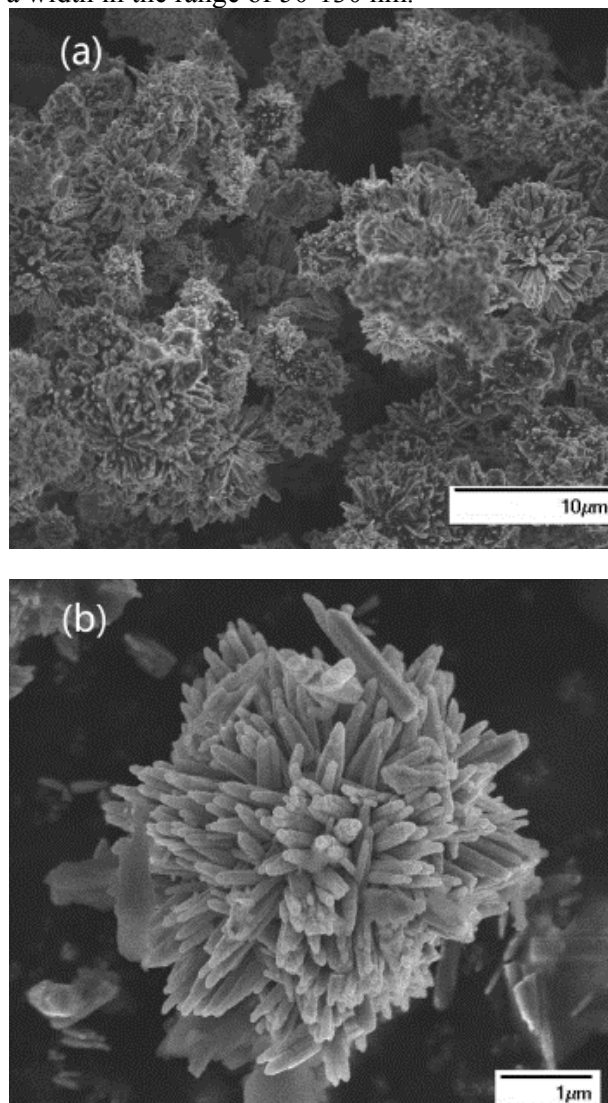


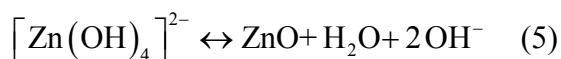
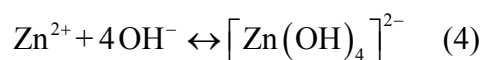
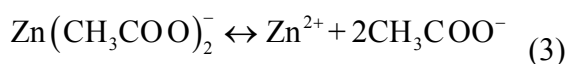
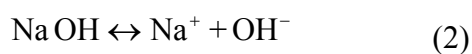
Fig.2. SEM images of synthesized ZnO nanostructures, (a) Low magnification, and (b) high magnification images of ZnO with flower-like morphology

Growth mechanism

Previous reports indicated that the formation process of ZnO nanostructures in alkali medium, the size, dimension and morphology of the final products were affected by external conditions such as temperature, complexing

agent and pH value of the solution during the hydrothermal process [26-27].

The possible formation mechanism of flower-like ZnO is proposed based on the investigation results. Firstly, the formation of primary ions have been shown in Eqs.(1-3). With the increasing of NaOH, the excess OH⁻ ions are in favor of the formation of [Zn(OH)₄]²⁻ ions which further decomposes to give ZnO nanoparticles (Eq.4). A part of [Zn(OH)₄]²⁻ ions will directly transform into ZnO nuclei after the concentration above its critical solubility under hydrothermal conditions (Eq.5) [28].



Based on surface energy minimization, the ZnO crystallites from zinc hydroxyl nucleate are beneficial for lifting the growth rate of ZnO nuclei along the c-axis direction and then grow into 1D nanorods. When the precursor concentration increases, the nucleation of ZnO is so rapid that more ZnO nuclei form in the initial stage. These nuclei may aggregate together due to excess saturation. Each of them individually grows along the c-axis into rod-like crystal, and thus flower-like architectures are finally formed [29]. The possible growth mechanism has been illustrated in Fig.3.

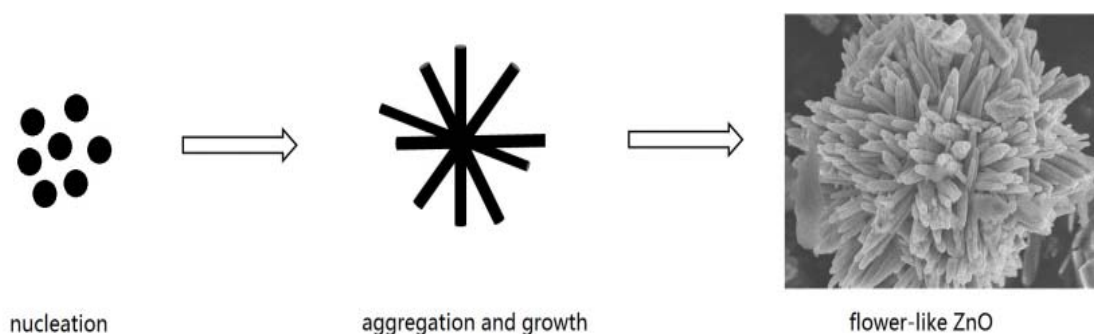


Fig.3. The schematic illustration of the possible growth process for flower-like ZnO nanostructures

Room temperature photoluminescence studies

The room temperature photoluminescence (PL) spectrum of the as-synthesized ZnO nanostructures is shown in Fig.4. It can be seen that the PL spectrum is composed of two emission bands: a weak emission band in violet region (381 nm) and a strong emission band in visible region. In general, the UV peak at room temperature is attributed to the recombination of free excitons [30-32]. The visible emission band of flower-like ZnO microstructures is ranging from 450 nm to 750 nm. This emission is ranging from green to red is quite complicated due to the native and dopant-

induced defects in ZnO, which are sensitively related to the synthesis procedures [33]. The possible intrinsic 'native' deep levels in ZnO are oxygen vacancy (V_{O}), zinc vacancy (V_{Zn}), oxygen interstitial (O_i), zinc interstitial (Zn_i), oxygen anti-site (O_{Zn}), and zinc anti-site (Zn_o). The green emission at 540 nm (2.30 eV) are attributed to the interstitial oxygen (O_i) [33]. The peak at 600 nm (2.07 eV) are possibly caused by the monovalent vacancies of zinc (V_{Zn}^+) and oxygen (V_{O}^-) in ZnO [33-34]. The result shown that flower-like ZnO possess a high-quality crystal and few oxygen vacancies.

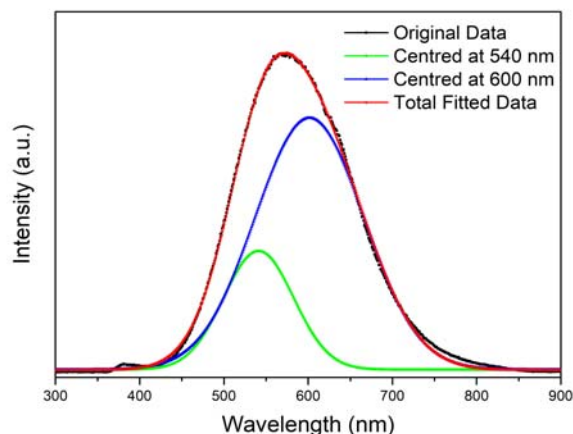


Fig.4. Room temperature photoluminescence spectrum of the as-synthesized ZnO nanostructures

CONCLUSIONS

In summary, flower-like ZnO nanostructures have been successfully synthesized by hydrothermal method with zinc acetate dehydrate ($\text{Zn}(\text{CH}_3\text{COO})_2 \cdot 2\text{H}_2\text{O}$) and sodium hydroxide (NaOH). The as-synthesized ZnO nanostructures were characterized by X-ray diffraction (XRD), scanning electron microscopy (SEM), and room temperature photoluminescence (PL) spectra. The results indicate that the samples are highly crystalline with the wurtzite hexagonal phase. The Photoluminescence spectrum (PL) showed that the as-synthesized flower-like ZnO showed ultraviolet emission (UV) at 381 nm and the visible emission band ranging from 450 nm to 750 nm, respectively. The UV peak at room temperature is attributed to the recombination of free excitons and the visible emission band ranging from green to red is attributed to the interstitial oxygen (O_i) and the monovalent vacancies, respectively.

ACKNOWLEDGEMENTS

This research was financially supported by the Fundamental Research Funds for the Central Universities (2018MS042) and China Scholarship Council (CSC).

NOMENCLATURE

XRD - X-ray diffraction;
SEM - scanning electron microscopy;
PL - photoluminescence;

3D - three-dimension;
UV - ultraviolet emission;
ZnO - Zinc oxide;
CVD - chemical-vapor deposition;
MBE - molecular-beam epitaxy;
PLD - pulsed-laser deposition;
 $\text{Zn}(\text{CH}_3\text{COO})_2 \cdot 2\text{H}_2\text{O}$ - zinc acetate dehydrate;
NaOH - sodium hydroxide;
RT-PL - Room temperature photoluminescence;
 V_O - oxygen vacancy;
 V_Zn - zinc vacancy;
 O_i - oxygen interstitial;
 Zn_i - zinc interstitial;
 O_Zn - oxygen anti-site;
 Zn_O - zinc anti-site.

REFERENCES

- [1] D.C. Look, Doping and Defects in ZnO, 1st ed., Elsevier Ltd., UK, 2006.
- [2] B.A. Buchine, W.L. Hughes, F.L. Degertekin, Z.L. Wang, Bulk acoustic resonator based on piezoelectric ZnO belts. *Nano Letter* **6**, 1155-1159 (2006).
- [3] M. Willander, O. Nur, Q.X. Zhao, L.L. Yang, M. Lorenz, B.Q. Cao, J. Zuniga Perez, C. Czekalla, G. Zimmermann, M. Grundmann, A. Bakin, A. Behrends, M. Al-Suleiman, A. Al-Shaer, A. Che Mofor, B. Postels, A. Waag, N. Boukos, A. Travlos, H.S. Kwack, J. Guinard, D. Le Si Dang, Zinc oxide nanorod based photonic devices: recent progress in growth, light emitting diodes and lasers. *Nanotechnology* **20**, 332001 (2009).
- [4] M. Laurenti, S. Porro, C. Pirri, C. Ricciardi, A. Chiolerio, Zinc oxide thin films for memristive devices: a review. *Critical Reviews in Solid State and Materials Sciences*, **42** (2), 153-172 (2017).
- [5] J.J. Cole, X. Wang, R.J. Knuesel, H.O. Jacobs, Integration of ZnO microcrystals with tailored dimensions forming light emitting diodes and UV PV cells. *Nano Letter* **8**(5), 1477-1481 (2008).
- [6] S. H. Bhang, W. S. Jang, J. Han, J. Yoon, W. La, E. Lee, Y.S. Kim, J. Shin, T. Lee, H.K. Baik, B. Kim. Zinc oxide nanorod-based piezoelectric dermal patch for wound healing. *Advanced Functional Materials*, **27** (1). (2017).
- [7] Q. Zhang, T.P. Chou, B. Russo, S.A. Jenekhe, G. Cao, Aggregation of ZnO nanocrystallites for high conversion efficiency in dye-sensitized solar cells. *Angew. Chemie Int. Ed.* **47**, 2402-6 (2008).
- [8] J.Y. Kim, H. Jeong, D.J. Jang, Hydrothermal fabrication of well-ordered ZnO nanowire arrays on Zn foil: room temperature ultraviolet nanolasers. *Journal of Nanoparticle Research* **13**, 6699-6706 (2011).
- [9] Z.L. Wang, J. Song, Piezoelectric Nanogenerators Based on Zinc Oxide Nanowire Arrays. *Science* **312**, 242-246 (2006).

- [10] T.L. Phan, S.C. Yu, R. Vincent, N.H. Dan, W.S. Shi, Photoluminescence properties of various CVD-grown ZnO nanostructures. *Journal of Luminescence* **130**, 1142-1146 (2010).
- [11] B. Daragh, F.A. Rabie, B. Teresa, G.R. David, T. Brendan, O.H. Martin, M. Enda, Study of Morphological and Related Properties of Aligned Zinc Oxide Nanorods Grown by Vapor Phase Transport on Chemical Bath Deposited Buffer Layers. *Crystal Growth & Design* **11** 5378-5386 (2011).
- [12] I.C. Robin, P. Marotel, A.H. El-Shaer, V. Petukhov, A. Bakin, A. Waag, M. Lafossas, J. Garcia, M. Rosina, A. Ribeaud, S. Brochen, P. Ferret, G. Feuillet, Compared optical properties of ZnO heteroepitaxial, homoepitaxial 2D layers and nanowires. *Journal of Crystal Growth* **311** 2172-2175 (2009).
- [13] Z.Q. Wang, X.D. Liu, J.F. Gong, H.B. Huang, S.L. Gu, S.G. Yang, Epitaxial growth of ZnO nanowires on ZnS nanobelts by metal organic chemical vapor deposition. *Crystal Growth & Design* **8**, 3911-3913 (2008).
- [14] B.A. Taleatu, A.Y. Fasasi, G. Di Santo, S. Bernstorff, A. Goldoni, M. Fanetti, L. Floreano, P. Borghetti, L. Casalis, B. Sanavio, C. Castellarin-Cudia, Electro-chemical deposition of zinc oxide nanostructures by using two electrodes. *AIP Advances* **1**, 032147 (2011).
- [15] M.J. Height, L. Mädler, S.E. Pratsinis, Nanorods of ZnO made by flame spray pyrolysis. *Chemistry of Materials* **18**, 572-578 (2006).
- [16] R.J. Mendelsberg, M. Kerler, S.M. Durbin, R.J. Reeves, Photoluminescence behavior of ZnO nanorods produced by eclipse PLD from a Zn metal target. *Superlattices and Microstructures* **43**, 594-599 (2008).
- [17] J.B. Shen, H.Z. Zhuang, D.X. Wang, C.S. Xue, H. Liu, Growth and Characterization of ZnO Nanoporous Belts. *Crystal Growth & Design* **9**, 2187-2190 (2009).
- [18] L.B. Feng, A.H. Liu, M. Liu, Y. Ma, J. Wei, B.Y. Man, Fabrication and characterization of tetrapod-like ZnO nanostructures prepared by catalyst-free thermal evaporation. *Materials Characterization* **61**, 128-133 (2010).
- [19] H. Zhang, D.R. Yang, X.Y. Ma, Y.J. Ji, J. Xu, D.L. Que, Synthesis of flower-like ZnO nanostructures by an organic-free hydrothermal process. *Nanotechnology* **15**, 622-626 (2004).
- [20] S. Chakraborty, A.K. Kole, P. Kumbhakar, Room temperature chemical synthesis of flower-like ZnO nanostructures. *Materials Letters* **67**, 362-364 (2012).
- [21] X.X. Yang, W. Lei, X.B. Zhang, B.P. Wang, C. Li, K. Hou, Y.K. Cui, Y.S. Di, Electrodeposition for antibacterial nickel-oxide-based coatings. *Thin Solid Films* **517**, 4385-4389 (2009).
- [22] X.T. Su, H. Zhao, F. Xiao, J.K. Jian, J.D. Wang, Synthesis of flower-like 3D ZnO microstructures and their size-dependent ethanol sensing properties. *Ceramics Int.* **38**, 1643-1651 (2012).
- [23] Y.H. Tong, Y.C. Liu, L. Dong, D.X. Zhao, J.Y. Zhang, Y.M. Lu, D.Z. Shen, X.W. Fan, Growth of ZnO nanostructures with different morphologies by using hydrothermal technique. *The J. of Phys. Chemistry B* **110**, 20263-7 (2006).
- [24] S.H. Jung, E. Oh, K.H. Lee, Y. Yang, C.G. Park, W.J. Park, S.H. Jeong, Sonochemical preparation of shape-selective ZnO nanostructures. *Crystal Growth & Design* **8**, 265-269 (2008).
- [25] W.W. Lee, J. Yi, S.B. Kim, Y.H. Kim, H.G. Park, W. Park, Morphology-controlled three-dimensional nanoarchitectures produced by exploiting vertical and in-plane crystallographic orientations in hydrothermal ZnO crystals. *Crystal Growth & Design* **11**, 4927-4932 (2011).
- [26] H. Zhang, D. Yang, S. Li, X.Y. Ma, Y. Ji, J. Xu, D. Que, Controllable growth of ZnO nanostructures by citric acid assisted hydrothermal process. *Materials Letters* **59**, 1696-1700 (2005).
- [27] C. Yan, D. Xue, L. Zou, A solution-phase approach to the chemical synthesis of ZnO nanostructures via a low-temperature route. *J. of Alloys and Compounds* **453**, 87-92 (2008).
- [28] R.X. Shi, P. Yang, X.B. Dong, Q. Ma, A.Y. Zhang, Growth of flower-like ZnO on ZnO nanorod arrays created on zinc substrate through low-temperature hydrothermal synthesis. *Applied Surface Science* **264**, 162-170 (2013).
- [29] W.Q. Peng, S.C. Qu, G.W. Cong, Z.G. Wang, Synthesis and structures of morphology-controlled ZnO nano- and microcrystals. *Crystal Growth & Design* **6**, 1518-1522 (2006).
- [30] J. Zhang, L. Sun, J. Yin, H. Su, C. Liao, C. Yan, Control of ZnO morphology via a simple solution route. *Chemistry of Materials* **14**, 4172-77 (2002).
- [31] M.H. Huang, Y.Y. Wu, H. Feick, N. Tran, E. Weber, and P.D. Yang, Catalytic growth of zinc oxide nanowires by vapor transport. *Advanced Materials* **13**, 113-116 (2001).
- [32] D. Zhang, X. Liu, Xin Wang, Growth and photocatalytic activity of ZnO nanosheets stabilized by Ag nanoparticles. *Journal of Alloys and Compounds* **509**, 4972-4977 (2011).
- [33] Y.W. Zhu, C.H. Sow, T. Yu, Q. Zhao, P.H. Li, Z.X. Shen, D.P. Yu, and Thong, J. T.-L. Thong, Co-synthesis of ZnO-CuO Nanostructures by Directly Heating Brass in Air. *Advanced Functional Materials* **16**, 2415-2422 (2006).
- [34] C. X. Xu, X. W. Sun, X. H. Zhang, L. Ke, and S. J. Chua, Zinc oxide nanowires and nanorods fabricated by vapour-phase transport at low temperature. *Nanotechnology* **15**, 856-861 (2004).